Young's Modulus of Nanoconfined Liquids?

First author: Shah Haidar Khan[1]
[1]*Department of Physics, University of Peshawar, Peshawar, 25120, Pakistan*

Second/Corresponding author: Peter Manfred Hoffmann[2]
[2]*Department of Physics and Astronomy, Wayne State University, Detroit, Michigan 48201, USA*

Abstract

In material science, bioengineering, and biology, thin liquid films and soft matter membranes play an important role in micro-lubrication, ion transport, and fundamental biological processes. Various attempts have been made to characterize the elastic properties, such as Young's modulus, of such films using Hertz theory by incorporating convoluted mathematical corrections. We propose a simple way to extract tip-size independent elastic properties based on stiffness and force measurement through a spherical tip on a flat surface. Using our model, the Young's moduli of nanoconfined, molecularly-thin layers of a model liquid TEHOS (tetrakis 2-ethylhexoxy silane) and of water were determined using a small-amplitude AFM. This AFM can simultaneously measure the stiffness and forces of nanoscale films. While the stiffness scales linearly with the tip radius, the measured Young's modulus essentially remains constant over an order of magnitude variation in the tip radius. The values obtained for the elastic modulus of TEHOS and water films on the basis of our method are significantly lower than the confining surfaces' elastic moduli, in contrast with the uncorrected Hertz model, suggesting that our method can serve as a simple way to compare elastic properties of nanoscale thin films as well as to characterize a variety of soft films. In addition, the elastic properties (elastic modulus) of nanoconfined liquid films seem to remain fairly independent of increasing confinement.

Keywords: Young's modulus; nanoconfined liquids; small-amplitude AFM; TEHOS (tetrakis 2-ethylhexoxy silane); water; soft films

Nanoconfined liquids play important role in geology [1], engineering [2], medicine [3, 4], biophysics [5-7], nanotribology [8, 9] and other branches of science and technology [10]. The viscoelastic properties of nanoconfined water are particularly important because of its role as the matrix of life and in shaping our planet. When confined, water and other liquids form ordered molecular layers against atomically smooth surfaces [11-15]. This molecular layering gives rise to changes in elastic as well as viscous properties of the confined liquids. While the changes in viscous properties remain highly controversial [13, 14, 16-23], the changes in elastic properties (stiffness) of liquids upon confinement are widely observed and established [14, 15, 19, 24, 25].

Sophisticated tools such as the atomic force microscope (AFM) and surface forces apparatus (SFA) can measure changes in the mechanical properties of liquids confined at the nanoscale. AFM has also been used to measure stiffness of thin biological samples [5, 7, 26]. Although the stiffness of a nanoconfined liquid film is supposed to increase with decrease in thickness of the film [14, 19-21, 27], it is not straightforward to compare measurements taken under different conditions. One of the factors camouflaging the true elastic properties of nanoconfined films in AFM experiments is the tip geometry. The elastic properties such as stiffness of nanoconfined liquid films have been found to vary linearly with the radius of the tip [21], as expected from the Derjaguin approximation [28].

Calculating a property such as elastic modulus may not seem to make sense because of the difficulty in calculating the thickness and indentation depth in nanoconfined films. However, efforts have been made in the past to measure elastic modulus of ultrathin films. Unfortunately, these models are highly mathematical and/or limited to soft films (gels) [5, 7, 29]. For example, corrections have been proposed toward improving the applicability of the Hertz contact model to microfilms of biological samples and to addressing difficulties in determining the contact point between the tip and the substrate. In a recent study, efforts were made to correctly measure the Young's modulus of gel substrates used to support cells by atomic force microscopy (AFM) [7]. Corrections were made to address the infinite size of the substrates inherent in Hertz theory and to incorporate the non-linearity of the material using the finite-element method [7]. We propose an alternate to Hertz theory, which may be helpful toward standardization of elastic properties of nanoconfined liquid films and microgels. This approach allows us to determine an effective elastic modulus for a nanoconfined liquid film. We apply this method to nanoconfined TEHOS (tetrakis 2-ethylhexoxy silane), an inert model liquid with spherical molecular shape of a diameter close to 1 nm [30-33], as well as to water. We have studied TEHOS previously [21, 32]. We compare the elastic modulus of TEHOS obtained with different sized probes and show that the effect of tip geometry can be accounted for. We also compare our results based on the proposed model with those obtained using Hertz theory. Our results for the elastic modulus show that using Hertz theory greatly exaggerates elastic properties of thin films, as has been already suggested elsewhere [5, 7]. We also determine the elastic modulus for nanoconfined water films and compare it with TEHOS to highlight the qualitative/quantitative difference between the two.

For water calculations, we have used previous measurements [15, 20] applying an improved analysis of the data.

Theory

In the following, we compare our model with conventional Hertz theory.

1. Our Model

The elastic modulus (Young's modulus) is a property that represents how much resistance an object offers to being elastically deformed along an axis under the application of a force. If $d\sigma$ is applied uniaxial stress and $d\epsilon$ is resulting strain, the elastic modulus of the contact can be written as:

$$E_c = \frac{d\sigma}{d\varepsilon} \qquad (1)$$

The geometry of a hemisphere and a flat surface can be used to model the AFM cantilever tip and a substrate in contact through a liquid film of thickness z, as shown in Figure 1. Let us suppose A is the effective contact area and z the separation between the tip apex and the substrate along which the compressive force is applied. If F is the loading force, the increment in stress can be written as $d\sigma=dF/A$, and the increment in linear strain as $d\varepsilon=dz/z$. Equation (1) can thus be written as:

$$E_c = \frac{dF / A}{dz / z} = \frac{dF}{dz}(z / A) = k(z / A), \qquad (2)$$

where $k = dF/dz$ is the interaction stiffness of the sample. Equation 1 is basically Hook's law considering linear characteristics of a spring. As such, it may not be applied to the entire thickness of a nanonconfined film in which the stiffness usually increases nonlinearly with decrease in thickness of the film [14, 19-21, 31]. Our model assumes the linear spring characteristics for very small intervals of compression steps (e.g. 0.18 Å in the case of water, less than the molecular size by an order of magnitude) and calculates the stiffness without seriously violating the linearity approximation. The equation described elsewhere [14, 27] is used to measure the value of stiffness during each such step.

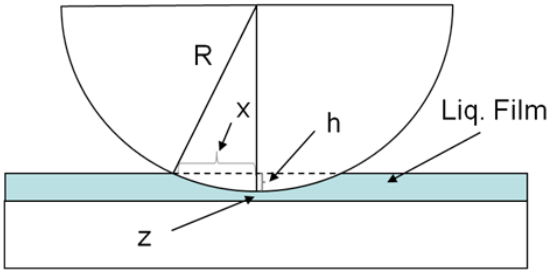

Figure 1. A tip of assumed hemispherical shape of radius R and a planar substrate confining a liquid. x represents the radius of the effective contact area, A; h is the indentation depth in the stiff liquid layer of a few molecular dimension; and z is the film thickness (the distance between the planar substrate and the tip apex).

With the help of Figure 1, we can find a relationship between the effective contact area and the radius of the sphere [34]. If R is the radius and h is the indentation depth, the effective contact area A can be replaced by πx^2 such that:

$$A = \pi x^2 = \pi(R^2 - (R-h)^2) = \pi(2R-h)h \quad (3)$$

Using equation (3) in equation (2), we obtain:

$$E_c = \frac{k\ z}{\pi(2R-h)h} \quad (4)$$

In the limit $h<<R$, the above equation can be written as follows.

$$E_c = \frac{kz}{2\pi Rh} \quad (5)$$

Equation (5) should give the effective elastic modulus of the interacting sample liquid. As the interaction stiffness k scales linearly with the tip radius R [21], the elastic modulus dependence upon the tip radius R cancels out. The above equation can, in principle, be used to extract tip-independent elastic properties of the confined liquid film. Here, we neglected the effects of elastic flattening of the confining surfaces [35] due to our small tips (radii~micrometer) and small measurement amplitudes (<1nm).

In order to determine the indentation depth, h, we propose an approach based on the principle of equilibrium. The indentation h can be calculated by using the applied force in equilibrium with other forces giving rise to stiffness of the confined liquid film:

$$h = \frac{k_L d}{k} = \frac{F}{k} \quad (6)$$

Here, k_L is the stiffness of the cantilever, d is its deflection (bending), and k is the stiffness of the the confined liquid film. For a compressional speed less than one nm/s and a vibration amplitude smaller than the size of the molecules, the sample compressed by a cantilever tip in an AFM experiment can be regarded as being in quasi-mechanical equilibrium.
With this, we arrive at the following expression for the effective elastic modulus based on the measured interaction stiffness, cantilever bending, and tip-surface distance:

$$E_c = \frac{k^2 z}{2\pi RF} \quad (7)$$

Because both the force, F, and the stiffness, k, are needed to determine the elastic modulus, an AFM technique that can simulateneously measure both parameters is needed. In our case, this is achieved by superimposing a small, sub-molecular dither on the cantilever, and measuring the stiffness [14, 15, 20, 27] and the static deflection/bending of the cantilever, simultaneously.

2. Hertz Model

A conventional Hertzian approach, on the other hand, will give the effective elastic modulus of the contact, but because of the infinitesimal size of the liquid film or biological microgel, will be dominated by substrate effects. Many corrections have been proposed to justify its use in the case of microgels [5, 7, 26]. For the sake of comparison, we briefly describe the Hertz model in its primitive form. The model assumes infinitely thick samples [5, 7]; and, therefore, the formula does not provide results representative of thin films. In AFM, the indenter's Young modulus is much higher than the sample. The effective elastic modulus E_c is thus determined only by the Young's modulus of the sample and its Poisson's ratio [36, 37]:

$$E_c = \frac{E}{1-\nu^2} \tag{8}$$

Also, the normal force between two bodies in contact can be written as follows [37, 38].

$$F = \frac{4}{3}\left(\frac{E}{1-\nu^2}\right)R^{\frac{1}{2}}h^{\frac{3}{2}} = \frac{4}{3}E_c R^{\frac{1}{2}}h^{\frac{3}{2}}$$

The stiffness k can be written as

$$k = \frac{dF}{dh} = 2E_c R^{\frac{1}{2}}h^{\frac{1}{2}} \tag{9}$$

$$E_c = \frac{k}{2\sqrt{Rh}}$$

Again using equation 6, we can write the above equation as follows:

$$E_c = \frac{k^{3/2}}{2\sqrt{RF}} \tag{10}$$

Equation 10 gives the formula based on Hertz model. It does not contain the film thickness, z, and depends on the square root of the tip radius providing incorrect scaling with the tip radius.

Experimental

A home-built AFM using an optical fiber Fabry-Perot interferometer to monitor the cantilever vibration was used for the measurement of phase and amplitude [27]. Our AFM has three-stage vibration and two-stage acoustic insulation [15]. The cantilevers were vibrated well below resonance frequency with amplitude smaller than the molecular size of the liquid to insure linearity. Our AFM is sensitive enough to provide better than 0.01 nm vertical resolution for force distance curves. Four different cantilevers of stiffness 55 N/m, 35, 2.4 N/m and 1.0 N/m were used (Figure 3). The stiffness of the cantilevers was determined using the geometrical method as well as the thermal method [39].The radii of the tips were 19 μm, 6 μm, 0.9 μm and 0.5 μm, respectively. Polished silicon wafers (100) were used as substrates. The cantilever was completely immersed in the liquid during measurement and the liquid located between the tip and a flat substrate constituted the confined liquid film. The silicon substrates were oxidized in

Piranha solution at 100°C for about one hour to clean them from contaminants. The cantilevers were first rinsed with acetone and then ethanol for about five minutes. All the levers and substrates were finally rinsed well with de-ionized water (resistivity 18 MΩ-cm) from a Siemens (formerly USFilter) PURELAB classic UV/UF system, and dried overnight in an oven at 100°C. We used Fisher brand micropipettes to deliver the liquid to the liquid cell. The micropipettes were soaked in concentrated HCl overnight before rinsing them with clean water. The glass dishes were kept in saturated NaOH isopropanol solution for about 10 hours, to make them sufficiently hydrophilic and clean, and washed in ultrapure water before use. TEHOS was purchased from Gelest, Inc. The usual compression rates of the liquid were less than 1 nm/s. The operational frequencies of the cantilevers ranged from 300 to 900 Hertz. The measurements on water were performed using freshly-cleaved mica surface as substrate.

Figure 2 shows the SEM images of the four tips used in the measurement of interaction stiffness and elastic modulus of TEHOS films. Overall, we performed 50 successful measurements out of a total of about 300. A measurement was considered successful if 1; the stiffness curve shows well defined molecular size oscillations clearly distinguishable from noise and 2; the force curve shows static deflection of the cantilever without significant drag. All tips are shown on a scale of 100 μm to ease comparison. We used SEM imaging (at higher resolution) to determine the effective radius of the tips for our analysis. The tip in Figure 2(b) was also used to measure the stiffness and the elastic modulus of pure water (18 MΩ-cm).

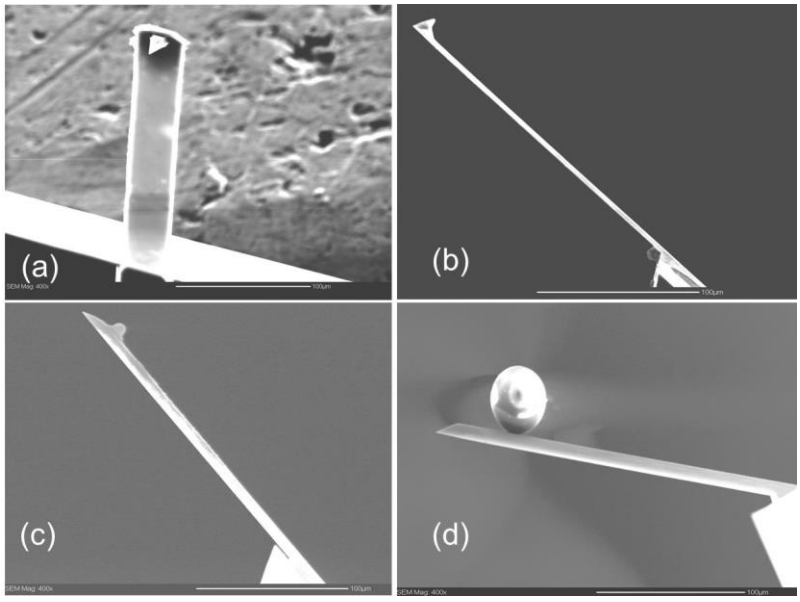

Figure 2. SEM images of surfaces of the four tips on a scale of about 100 micrometer. The radii of the tips are (a) 0.5 μm (b) 0.9 μm (c) 6 μm and (d) 19 μm.

It is challenging in atomic force microscopy measurements to measure the confinement size or sample thickness. We measured the amplitude, phase, and the average photodiode signal corresponding to the deflection of the cantilever. By a strong change in the slope of the photodiode signal, a large reduction in the amplitude of the cantilever, and a significant phase change, the tip-surface contact point could be clearly discerned in about 30 % of measurements, which were the measurements chosen for further analysis.

Results

Representative figures of the measured stiffness (Figure 3a) and elastic modulus (Figure 3b) of nanoconfined TEHOS film are shown in Figure 3. The elastic modulus calculated using equation 7 (our model) and equation 10 (Hertz model) are represented by hollow circles and filled circles, respectively. The substrate lies to the right of the figure at the origin. The stiffness was calculated as $k = k_L\left(\frac{A_{0Cos\varphi}}{|A|} - 1\right)$ using our small-amplitude dynamic AFM [14, 27]. Here, A_0 is the drive amplitude of the cantilever, A is the measured amplitude as the surface is approached, k_L is the lever stiffness, and φ is the phase of the cantilever tip. The stiffness oscillations as shown in Figure 3a are expected to result from ordering of the molecules along the silicon substrate. The spacing between stiffness peaks resulting from ordering of the molecules is comparable to the size of TEHOS molecules (1nm). In Figure 3b, the Hertz elastic modulus is orders of magnitude higher than our elastic modulus. The Hertz theory gives elastic modulus in GPa close to the elastic modulus of silicon, which is the substrate.

-

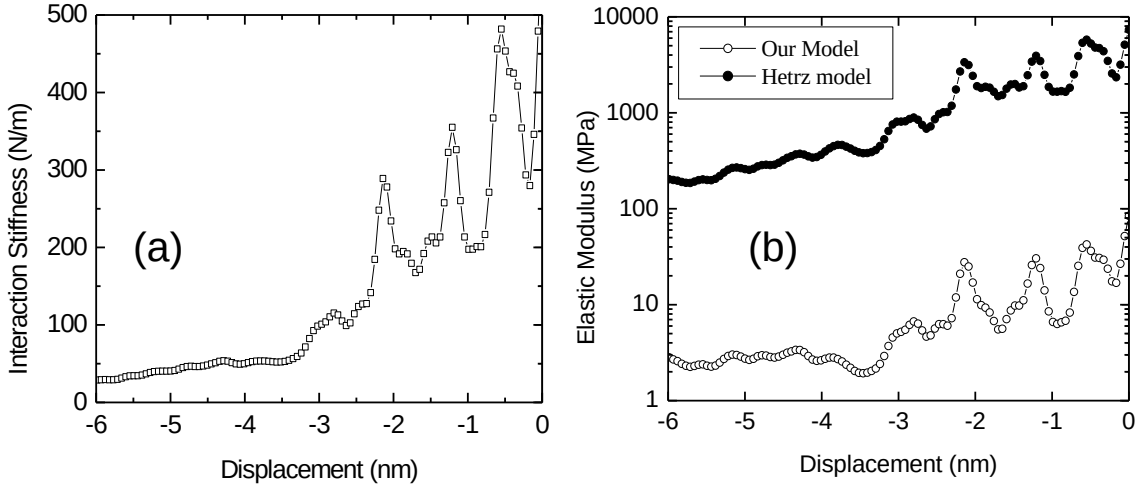

Figure 3. (a) The stiffness of the confined film as a function of displacement. The substrate lies to the right of the plot at zero nanometer. (b) The elastic modulus according to our model (hollow circles) and according to Hertz theory (filled circles).

Figure 4 shows the elastic modulus as a function of the number of confined molecular layers of TEHOS. The values are an average of all the measurements taken over four significantly different size tips. The elastic modulus is plotted on a logarithmic scale to accommodate both the models (the Hertz model and our model) on the same plot. As shown by the filled circles, the Hertz model gives an elastic modulus above 10^9 Pascal, which is not physical taking into consideration soft samples or liquids. This value is close to the elastic moduli of solid materials such as silicon or mica. However, the elastic modulus calculated on the basis of our model, the filled squares, is of the order of 10^7 Pascal i.e. about two orders of magnitude smaller than the value given by Hertz theory. Compared with a couple of existing reports about elastic modulus of thin films, our values are significantly higher [5, 7]. This difference in elastic modulus may be due to the orders of magnitude difference in the thickness of the films and/or the highly spongy nature of the material, Poly (vinyl alcohol) (PVA) gels [5], as compared with our incompressible liquids. In some cases, our values are generally comparable to already measured (for adsorbed water layer) [40] or projected values [29].

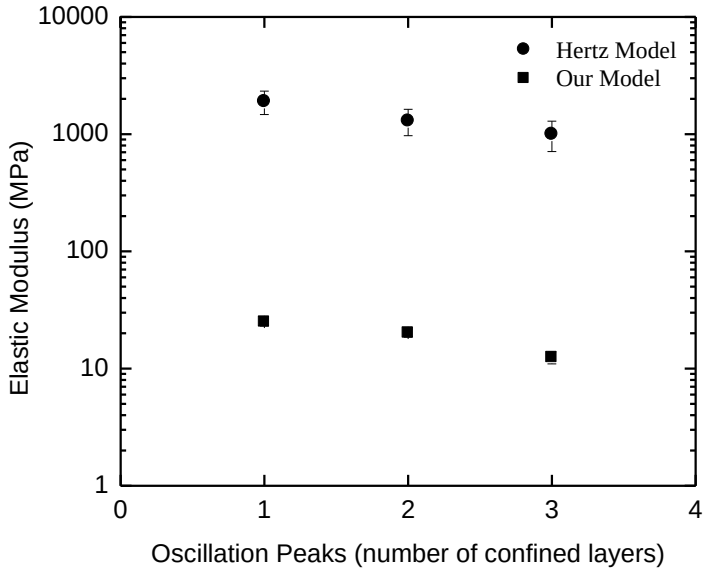

Figure 4. Elastic modulus as a function of the number of confined molecular layers of TEHOS. The points in the data correspond to the ordered state of molecular layers under confinement.

To see the dependence of the elastic modulus on the size of the tips, we plotted the elastic modulus and stiffness against the radii of the tips. Figure 5 (a, b) shows how (a) the stiffness and (b) the elastic modulus of nanoconfined TEHOS film vary with the size of the tip. The stiffness and the elastic modulus are represented on a logarithmic scale to help comparing the two quantities' dependence on the tip size. In the case of stiffness (Figure 5a), the solid line is a best fit to the variation of the peak values (solid squares), when a single molecular layer is confined. The dashed line represents a best fit to the peaks when two layers are confined (solid spheres), and the dotted line is the best fit when three layers are enclosed (solid triangles). All the best fit

lines have nearly the same slope (=1.1), indicating a linear relationship between the stiffness and the tip size (radius) [21]. In contrast, the elastic modulus (Figure 5b) remains essentially constant over the tip radii ranging from 0.5 to 19 μm. The slope of the three straight line fits, the solid line (solid squares) corresponding to one confined layer, the dashed line (solid circles) corresponding to two confined layers, and the dotted line (solid triangles) corresponding to three confined layers, ranged from 0.1 to 0.2. It shows a reasonably constant profile of the elastic modulus with the tip size. The slight increase toward higher radii may be the result of jamming of the molecules during squeeze-out more likely for larger tips [41]. However, more experimental efforts are required to pinpoint the mechanism behind it. The next step would be to calibrate more accurately the tip shape on a finer scale to minimize the errors in tip geometry permeating into stiffness and force measurements.

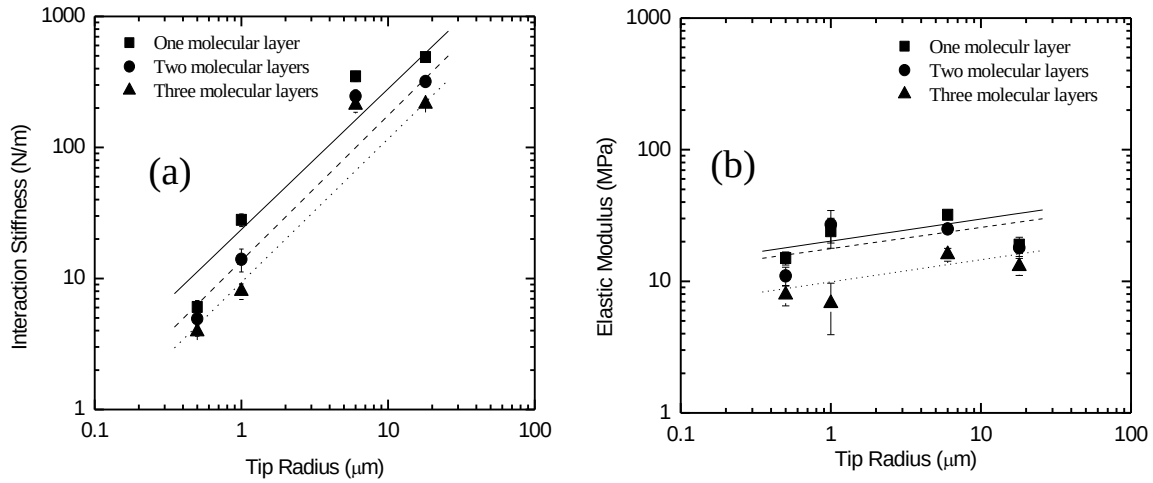

Figure 5. (a) The interaction stiffness of nanoconfined TEHOS as function of the tip radius. The three lines, solid, dashed, and dotted, are best fits to the first (squares), second (circles) and third (triangles) stiffness oscillation peaks off the substrate surface. The slope of the lines is about 1.1. (b) The elastic modulus as a function of the tip radius. The three lines are the best fit to the elastic modulus values of the peaks mentioned in (a). The slope of the elastic modulus lines is 0.1-0.2.

The above discussion shows that the elastic modulus can be regarded as a material dependent quantity fairly independent of tip radius (Figure 5b). It is therefore tempting to calculate the elastic modulus for other liquids. We calculated the elastic modulus for ultrapure (18 MΩ-cm) nanoconfined water using equation 7 with the tip shown in Figure 2b (radius = 0.9 μm). Figure 6 shows a comparison between the elastic modulus for TEHOS and deionized water plotted on a logarithmic scale as a function of the film thickness (the number of confined molecular layers). The data points correspond to the peak values of the elastic modulus oscillations as the tip

approaches the substrate. The solid squares in Figure 6 represent the peak elastic modulus of layer 1 (the closest to the substrate), 2 and 3 of nanoconfined TEHOS averaged over all the tip radii. The solid circles overlapping the solid squares represent the peak values of the elastic modulus of TEHOS measured with the tip of radius 0.9 μm (Figure 6). The same tip was used to measure the elastic modulus of water film (solid triangles). It is worth noting that the elastic modulus of water, a significantly thinner film due to the smaller molecular size, is much smaller (by an order of magnitude) than that of TEHOS. Quantitatively, the elastic modulus of water presented here is similar to a recently reported study, which mainly describes the maximum pressure that the adsorbed water layer on mica can sustain [40]. The significantly higher elastic modulus of TEHOS may be attributed to the spherically symmetric hard shape of TEHOS molecules [30, 33] while the low elastic modulus of water may be due to fairly flexible molecules [34, 42, 43]. The lower elastic modulus of water may also be partially due to the presence of the adsorbed monolayer on the mica surface, which may allow partial slip at the boundary [44]. Our results of the elastic modulus of nanoconfined TEHOS and water are also comparable to a study that projected elastic modulus of soft film of about 500 nm thickness to be in the range of MPa [29]. The relatively higher elastic modulus layer 1 of water as compared with almost equal values of layer 2 and 3 may be indicative of the adsorbed water layer on mica [15, 40, 45-48].

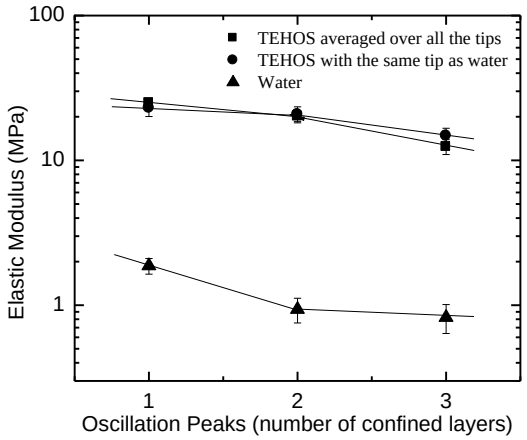

Figure 6. Comparison of the elastic modulus of TEHOS and water. The elastic modulus is given as a function of the number of confined molecular layers of nanoconfined TEHOS, and water, averaged over all the tips used. The lines joining the data points are a guide to the eye, and do not show any functional significance. Quantitatively, the value of the first layer is closer to the pressure sustainability [40]of a recently reported adsorbed monolayer [15].

In Figure 6, the elastic modulus of TEHOS film shows a fairly constant profile with the thickness. The same observation can be made about the sub-nanometer thick film of water, except the slightly high value associated with the monolayer [15] which may be the result of

stronger adhesion to the mica surface [40, 45, 48]. In general, the trend may suggest an important aspect of nanconcfined liquids: confinement does not significantly change the elastic properties of liquids.

Conclusion

The above discussion supports the validity of our simple method to measure elastic properties of thin films with the help of AFM, unaffected by the size of spherically symmetric tips. The measurement is possible by the use of a dynamic AFM that can measure force and stiffness simultaneously with amplitudes smaller than the size of the molecules. It can also be concluded that this method can be used for different nanoconfined liquids, allowing comparison. From our measurements on TEHOS and water, we found a large difference in modulus of these liquids when confined to 3 molecular layers or less. In addition, the results suggest slight or no dependence of the elastic modulus of liquids upon nanoconfinement. The next step will be to understand the mechanism behind the large difference in elastic modulus of TEHOS and water on the basis of their molecular properties. We hope that our simple method, while not perfect, may provide a new direction in profiling nanoconfined liquids on the basis of elastic properties. It may also be helpful in the measurement of elastic modulus of biological, as well as soft matter, films.

ACKNOWLEDGMENTS

P.M.H. would like to acknowledge funding through the National Science Foundation grant DMR 0804283, and through Wayne State University.

References

[1] Cheng, H., Hu, E. & Hu, Y. 2012 Impact of mineral micropores on transport and fate of organic contaminants: A review. *Journal of Contaminant Hydrology* **129–130**, 80-90. (doi:http://dx.doi.org/10.1016/j.jconhyd.2011.09.008).
[2] Marcus, P. & Mansfeld, F.B. 2005 *Analytical Methods In Corrosion Science and Engineering.* . 1st ed. Florida, USA, CRC Press, Taylor and Francis Group.
[3] Alessandrini, A. & Facci, P. 2005 AFM: a versatile tool in biophysics. *Measurement Science and Technology* **16**, R65.
[4] Wang, C., Ye, D.-K., Wang, Y.-Y., Lu, T. & Xia, X.-H. 2013 Insights into the "free state" enzyme reaction kinetics in nanoconfinement. *Lab on a Chip* **13**, 1546-1553. (doi:10.1039/C3LC41319E).
[5] Dimitriadis, E.K., Horkay, F., Maresca, J., Kachar, B. & Chadwick, R.S. 2002 Determination of elastic moduli of thin layers of soft material using the atomic force microscope. *Biophysical Journal* **82**, 2798-2810.
[6] Prakash, S., Pinti, M. & Bhushan, B. 2012 Theory, fabrication and applications of microfluidic and nanofluidic biosensors. *Philosophical Transactions of the Royal Society A: Mathematical, Physical and Engineering Sciences* **370**, 2269-2303. (doi:10.1098/rsta.2011.0498).
[7] Long, R., Hall, Matthew S., Wu, M. & Hui, C.-Y. 2011 Effects of Gel Thickness on Microscopic Indentation Measurements of Gel Modulus. *Biophysical Journal* **101**, 643-650. (doi:10.1016/j.bpj.2011.06.049).
[8] Bhushan, B., Israelachvili, J.N. & Landman, U. 1995 Nanotribology: friction, wear and lubrication at the atomic scale. *Nature* **374**, 607-616.
[9] Bocquet, L. & Charlaix, E. 2010 Nanofluidics, from bulk to interfaces. *Chemical Society Reviews* **39**, 1073-1095. (doi:10.1039/B909366B).
[10] Bhushan, B. 2007 *Springer Handbook of Nano-technology*. 2nd ed. New York, Springer.
[11] Israelachvili, J.N. & Pashley, R.M. 1983 Molecular layering of water at surfaces and origin of repulsive hydration forces. *Nature* **306**, 249-250.
[12] Bhushan, B., Israelachvili, J.N. & Landman, U. 1995 NANOTRIBOLOGY - FRICTION, WEAR AND LUBRICATION AT THE ATOMIC-SCALE. *Nature* **374**, 607-616.
[13] Antognozzi, M., Humphris, A.D.L. & Miles, M.J. 2001 Observation of molecular layering in a confined water film and study of the layers viscoelastic properties. *Applied Physics Letters* **78**, 300-302.
[14] Jeffery, S., Hoffmann, P.M., Pethica, J.B., Ramanujan, C., Ouml, zer, H., zg, uuml & Oral, A. 2004 Direct measurement of molecular stiffness and damping in confined water layers. *Physical Review B* **70**, 054114.
[15] Khan, S.H. & Hoffmann, P.M. 2015 Squeeze-out dynamics of nanoconfined water: A detailed nanomechanical study. *Physical Review E* **92**, 042403.
[16] Raviv, U. & Klein, J. 2002 Fluidity of Bound Hydration Layers. *Science* **297**, 1540-1543. (doi:10.1126/science.1074481).
[17] Zhu, Y. & Granick, S. 2003 Reassessment of solidification in fluids confined between mica sheets. *Langmuir* **19**, 8148-8151. (doi:10.1021/la035155+).
[18] O'Shea, S.J. 2006 Comment on "Oscillatory dissipation of a simple confined liquid". *Physical Review Letters* **97**, 179601 (doi:179601

10.1103/PhysRevLett.97.179601).
[19] Patil, S., Matei, G., Oral, A. & Hoffmann, P.M. 2006 Solid or liquid? Solidification of a nanoconfined liquid under nonequilibrium conditions. *Langmuir* **22**, 6485-6488. (doi:10.1021/la060504w).

[20] Khan, S.H., Matei, G., Patil, S. & Hoffmann, P.M. 2010 Dynamic Solidification in Nanoconfined Water Films. *Physical Review Letters* **105**, 106101-106105.
[21] Khan, S.H., Kramkowski, E.L., Ochs, P.J., Wilson, D.M. & Hoffmann, P.M. 2014 Viscosity of a nanoconfined liquid during compression. *Applied Physics Letters* **104**, 023110-023114. (doi:doi:http://dx.doi.org/10.1063/1.4861856).
[22] Labuda, A., Kobayashi, K., Suzuki, K., Yamada, H. & Grütter, P. 2013 Monotonic Damping in Nanoscopic Hydration Experiments. *Physical Review Letters* **110**, 066102.
[23] Beer, S.d., Otter, W.K.d., Ende, D.v.d., Briels, W.J. & Mugele, F. 2012 Non-monotonic variation of viscous dissipation in confined liquid films: A reconciliation. *EPL (Europhysics Letters)* **97**, 46001.
[24] Choe, H., Hong, M.H., Seo, Y., Lee, K., Kim, G., Cho, Y., Ihm, J. & Jhe, W. 2005 Formation, Manipulation, and Elasticity Measurement of a Nanometric Column of Water Molecules. *Physical Review Letters* **95**, 187801.
[25] Kim, B., Kwon, S., Mun, H., An, S. & Jhe, W. 2014 Energy dissipation of nanoconfined hydration layer: Long-range hydration on the hydrophilic solid surface. *Sci. Rep.* **4**, 6499-6505. (doi:10.1038/srep06499

http://www.nature.com/srep/2014/140930/srep06499/abs/srep06499.html#supplementary-information).
[26] Ahearne, M., Yang, Y., El Haj, A.J., Then, K.Y. & Liu, K.-K. 2005 Characterizing the viscoelastic properties of thin hydrogel-based constructs for tissue engineering applications. *Journal of The Royal Society Interface* **2**, 455-463. (doi:10.1098/rsif.2005.0065).
[27] Patil, S., Matei, G., Dong, H., Hoffmann, P.M., Karaköse, M. & Oral, A. 2005 A highly sensitive atomic force microscope for linear measurements of molecular forces in liquids. *Review of Scientific Instruments* **76**, 103705-103712. (doi:doi:http://dx.doi.org/10.1063/1.2083147).
[28] Derjaguin, B. 1934 Untersuchungen über die Reibung und Adhäsion, IV. *Kolloid-Zeitschrift* **69**, 155-164. (doi:10.1007/BF01433225).
[29] LEROY, S. & CHARLAIX, E. 2011 Hydrodynamic interactions for the measurement of thin film elastic properties. *Journal of Fluid Mechanics* **674**, 389-407. (doi:doi:10.1017/S0022112010006555).
[30] Yu, C.J., Richter, A., Datta, A., Durbin, M. & Dutta, P. 1999 <title>Observation of Molecular Layering in Thin Liquid Films Using X-Ray Reflectivity</title>. *Physical Review Letters* **82**, 2326-2329.
[31] Matei, G., Jeffery, S., Patil, S., Khan, S.H., Pantea, M., Pethica, J.B. & Hoffmann, P.M. 2008 Simultaneous normal and shear measurements of nanoconfined liquids in a fiber-based atomic force microscope. *Review of Scientific Instruments* **79**, 023706-023716. (doi:10.1063/1.2839913).
[32] Patil, S., Matei, G., Grabowski, C.A., Hoffmann, P.M. & Mukhopadhyay, A. 2007 Combined Atomic Force Microscopy and Fluorescence Correlation Spectroscopy Measurements to Study the Dynamical Structure of Interfacial Fluids. *Langmuir* **23**, 4988-4992. (doi:10.1021/la063745c).
[33] Yu, C.J., Richter, A.G., Datta, A., Durbin, M.K. & Dutta, P. 2000 Molecular layering in a liquid on a solid substrate: an X-ray reflectivity study. *Physica B: Condensed Matter* **283**, 27-31. (doi:http://dx.doi.org/10.1016/S0921-4526(99)01885-2).
[34] Israelachvili, J. 1992 *Intermolecular and Surface forces*. 2nd ed. San Deigo CA 92101, Academic Press Inc.
[35] Villey, R., Martinot, E., Cottin-Bizonne, C., Phaner-Goutorbe, M., Léger, L., Restagno, F. & Charlaix, E. 2013 Effect of Surface Elasticity on the Rheology of Nanometric Liquids. *Physical Review Letters* **111**, 215701-215706.
[36] Wenger, M.P.E., Bozec, L., Horton, M.A. & Mesquida, P. 2007 Mechanical Properties of Collagen Fibrils. *Biophysical Journal* **93**, 1255-1263. (doi:10.1529/biophysj.106.103192).
[37] Johnson, K.L. 1985 *Contact Mechanics*, Cambridge University Press.

[38] Campbell, C.S. 2006 Granular material flows – An overview. *Powder Technology* **162**, 208-229. (doi:http://dx.doi.org/10.1016/j.powtec.2005.12.008).
[39] Matei, G.A., Thoreson, E.J., Pratt, J.R., Newell, D.B. & Burnham, N.A. 2006 Precision and accuracy of thermal calibration of atomic force microscopy cantilevers. *Review of Scientific Instruments* **77**, 083703. (doi:doi:http://dx.doi.org/10.1063/1.2336115).
[40] Zhao, G., Tan, Q., Xiang, L., Cai, D., Zeng, H., Yi, H., Ni, Z. & Chen, Y. 2015 Structure and properties of water film adsorbed on mica surfaces. *The Journal of Chemical Physics* **143**, 104705. (doi:doi:http://dx.doi.org/10.1063/1.4930274).
[41] Beer, S., Otter, W.K., Ende, D., Briels, W.J. & Mugele, F. 2012 Can Confinement-Induced Variations in the Viscous Dissipation be Measured? *Tribology Letters* **48**, 1-9. (doi:10.1007/s11249-011-9905-4).
[42] Toukan, K. & Rahman, A. 1985 Molecular-dynamics study of atomic motions in water. *Physical Review B* **31**, 2643-2648.
[43] Schropp, B. & Tavan, P. 2010 Flexibility Does Not Change the Polarizability of Water Molecules in the Liquid. *The Journal of Physical Chemistry B* **114**, 2051-2057. (doi:10.1021/jp910932b).
[44] Neto, C., Evans, D.R., Bonaccurso, E., Butt, H.-J. & Craig, V.S.J. 2005 Boundary slip in Newtonian liquids: a review of experimental studies. *Reports on Progress in Physics* **68**, 2859.
[45] Cantrell & Ewing, G.E. 2001 Thin Film Water on Muscovite Mica. *The Journal of Physical Chemistry B* **105**, 5434-5439. (doi:10.1021/jp004305b).
[46] Cheng, L., Fenter, P., Nagy, K.L., Schlegel, M.L. & Sturchio, N.C. 2001 Molecular-Scale Density Oscillations in Water Adjacent to a Mica Surface. *Physical Review Letters* **87**, 156103.
[47] Leng, Y. & Cummings, P.T. 2006 Hydration structure of water confined between mica surfaces. *The Journal of Chemical Physics* **124**, 074711. (doi:doi:http://dx.doi.org/10.1063/1.2172589).
[48] Park, S.-H. & Sposito, G. 2002 Structure of Water Adsorbed on a Mica Surface. *Physical Review Letters* **89**, 085501.